

This discussion paper is/has been under review for the journal Climate of the Past (CP).
Please refer to the corresponding final paper in CP if available.

Tree-ring proxy based temperature reconstructions and climate model simulations: cross-comparison at the Pyrenees

I. Dorado Liñán^{1,2}, U. Büntgen³, F. González-Rouco⁴, E. Zorita^{5,6},
J. P. Montávez⁷, J. J. Gómez-Navarro⁷, M. Brunet⁸, I. Heinrich¹, G. Helle¹, and
E. Gutiérrez²

¹Helmholtz Centre Potsdam, German Centre for Geosciences, Climate Dynamics and Landscape Evolution, Potsdam, Germany

²University of Barcelona, Department of Ecology, Barcelona, Spain

³Swiss Federal Research Institute WSL, 8903 Birmensdorf, Switzerland

⁴Universidad Complutense de Madrid, Ciudad Universitaria, 28040 Madrid, Spain

⁵Helmholtz-Zentrum-Geesthacht, Geesthacht, Germany

⁶Bert Bolin centre for Climate Research, University of Stockholm, Sweden

⁷Departamento de Física, Universidad de Murcia, Murcia, Spain

⁸Centre for Climate Change, Universidad Rovira i Virgili, Tarragona, Spain

CPD

7, 3919–3957, 2011

Cross-comparison at the Pyrenees

I. Dorado Liñán et al.

[Title Page](#)

[Abstract](#)

[Introduction](#)

[Conclusions](#)

[References](#)

[Tables](#)

[Figures](#)

◀

▶

◀

▶

[Back](#)

[Close](#)

[Full Screen / Esc](#)

[Printer-friendly Version](#)

[Interactive Discussion](#)



Received: 19 October 2011 – Accepted: 27 October 2011 – Published: 17 November 2011

Correspondence to: I. Dorado Liñán (isabel@gfz-potsdam.de)

Published by Copernicus Publications on behalf of the European Geosciences Union.

Cross-comparison at the Pyrenees

I. Dorado Liñán et al.

[Title Page](#)

[Abstract](#)

[Introduction](#)

[Conclusions](#)

[References](#)

[Tables](#)

[Figures](#)

[|◀](#)

[▶|](#)

[◀](#)

[▶](#)

[Back](#)

[Close](#)

[Full Screen / Esc](#)

[Printer-friendly Version](#)

[Interactive Discussion](#)



Abstract

CPD
7, 3919–3957, 2011

May-to-September mean temperatures over the larger Pyrenees area (Northern Spain and Southern France) are reconstructed for the last Millennium from 22 maximum density (MXD) tree-ring chronologies. For the standardization of the tree-ring series, two detrending methods (Regional Curve Standardization (RCS) and 300-yr spline) were combined with and without an adaptive power transform (PT) for variance stabilization in the individual series. Thus, four different standardization procedures were applied to the data. Additionally, different regional chronologies were generated by computing a mean composite, averaging the local chronologies, or by applying Principal Components Analysis (PCA) to extract common variance from the subsets of individual MXD chronologies.

Calibration-verification trials were performed using the product of the three regional aggregation methods in split periods: 1900–1952 and 1953–2006. Two methods were used to calibrate the regional chronology: regression and a simple variance-matching, sometimes also known as composite-plus-scaling. The resulting set of temperature reconstructions was compared with climate simulations performed with global (ECHO-G over the last Millennium for the target region) and regional (MM5) climate models.

The reconstructions reveal inter-annual to multi-centennial temperature variations at the Pyrenees region for the last 750 yr. Generally, variations at inter-decadal timescales, including the cold periods associated with the solar minima, are common to all reconstruction variants although some discrepancies are found at longer timescales.

The simulations of the global circulation model ECHO-G and the regional model MM5 agree with the tree-ring based reconstructions at decadal to multi-decadal time-scales. However, the comparison also highlights differences that need to be understood, such as the amplitude of the temperature variations and the discrepancies regarding the 20th century trends.

[Title Page](#)

[Abstract](#)

[Introduction](#)

[Conclusions](#)

[References](#)

[Tables](#)

[Figures](#)

◀

▶

[Back](#)

[Close](#)

[Full Screen / Esc](#)

[Printer-friendly Version](#)

[Interactive Discussion](#)



1 Introduction

Estimations of future climate change indicate that variations in the global climate may have larger impacts at regional scales (IPCC, 2007). However, such forthcoming projections are hampered by the limited knowledge of the mechanism that gives rise to variability at multi-decadal and longer timescales due to the short length of instrumental records. The relative abundance of proxy records, mostly for temperature and precipitation, during the last millennium (e.g. Jones et al., 2009) offers the possibility to improve our understanding of past climate variability at interdecadal and longer time scales during this period (Jansen et al., 2007). Currently, two main approaches are being used to advance this line of research (Jansen et al., 2007; Jones and Mann, 2004; Mann et al., 2008): (1) creating new or extending the existing climate reconstructions back in time using documentary evidences or environmental proxies such as tree-ring parameters (width, density, isotopic content) corals, speleothems (Jones et al., 2009); and (2) simulations of natural and forced climate variability using climate models.

Tree-rings may contain useful information on past environmental conditions, which can be used to reconstruct past climate using statistical relationships to a target climate variable (Fritts, 1976; Cook and Kairiukstis, 1990). In this respect, tree-ring width and density are perhaps the most widely used proxies, and their relationships to seasonal temperatures have been extensively studied (Briffa, 2002, 2004; Büntgen et al., 2006, 2007, 2008; Esper et al., 2002, 2005a; Grudd, 2008). Although tree-ring measurements are accurately dated to the year, their ability to encode centennial to multicentennial climate variability is often limited by the standardization technique used to remove age-related trends in tree-ring time series. Thus, the climate signal at these timescales may be distorted by the technique used to remove non-climatic variations in tree-ring series (Cook et al., 1995; Esper et al., 2002, 2003; Briffa and Melvin, 2008). The Regional Curve Standardization has been suggested as an alternative technique with good performance to preserve low-frequency climate variations (Esper et al., 2002, 2004), although its strict sampling requirements significantly limit its implementation in

Cross-comparison at the Pyrenees

I. Dorado Liñán et al.

[Title Page](#)

[Abstract](#)

[Introduction](#)

[Conclusions](#)

[References](#)

[Tables](#)

[Figures](#)

[◀](#)

[▶](#)

[◀](#)

[▶](#)

[Back](#)

[Close](#)

[Full Screen / Esc](#)

[Printer-friendly Version](#)

[Interactive Discussion](#)



Cross-comparison at the Pyrenees

I. Dorado Liñán et al.

[Title Page](#)[Abstract](#)[Introduction](#)[Conclusions](#)[References](#)[Tables](#)[Figures](#)[|◀](#)[▶|](#)[◀](#)[▶](#)[Back](#)[Close](#)[Full Screen / Esc](#)[Printer-friendly Version](#)[Interactive Discussion](#)

practice and the effect of applying it to a suboptimal set of tree-ring data still requires further tests (Esper et al., 2003). In addition to standardization issues, the technique applied to estimate the reconstructed values also implies a challenge: whereas simple linear regression methods may underestimate low-frequency variability (Esper et al., 2005b; Zorita et al., 2010; McCarrol et al., 2011) variance-matching, in the following referred as scaling, shows better performance in retaining large scale variations but at the expense of inflated error estimates (Esper et al., 2005b; McCarrol et al., 2011)

A variety of climate models of increasing complexity is available for palaeoclimate simulations experiments, from energy balance models (EBM; Hegerl et al., 2006) to three-dimensional coupled ocean-atmosphere general circulation models (GCMs; Zorita et al., 2005). General circulation models have a global coverage, and produce complete 3-dimensional climate simulations, although their spatial resolution is still limited by computing power requirements. However the output of climate models depends on the characteristic of the model employed and on the prescribed external forcing, which are also estimated from proxy data (Jansen et al., 2007). Their validation is based on the assessment of their skill to reproduce the main characteristics of the current observed climate, although this does not guarantee their reliability to project future or past climate changes.

Alternatively, Regional Climate Models (RCM) simulate a limited area domain, thus reducing the computational requirements, which then allows for simulations of higher resolutions. Simulations with this kind of models for the last millennium have started to become available for specific regions in the last years (e.g. Gómez-Navarro et al., 2011a, b). This allows for more realistic model-data comparisons due to their improved resolution and characterization of land use categories, which permits a better representation of physical processes at regional scales.

Validations based on cross-comparisons between reconstructions and model estimates are still not common, especially at regional scales, despite offering the possibility to identify deficiencies in both approaches and thus to improve proxy based reconstructions, climate models and forcing estimates (e.g. D'Arrigo et al., 1999; Collins et

This work presents a temperature reconstruction for the Pyrenees region based on tree-ring density data. In addition, it also presents a comparison of the resulting palaeoclimate evidence with available GCM and RCM simulations over the area. The Pyrenees Range constitutes an interesting area for palaeoclimate reconstruction and simulations due to its location in the transition zones between two ecoclimatic regions (Eurasiberian and Mediterranean climate types) where future climate change is expected to have large effects (IPCC, 2007). The particular ecotonal location and the existence of old growth forest at their limit of natural distribution point to climate as the main driver of tree-growth. Indeed, temperature series have shown strong inter-site relationships between distant sites (Agustí-Panareda et al., 2000) pointing out the suitability of individual temperature sensitive tree-ring chronologies to be used in an ensemble regional temperature reconstruction. In accordance, Büntgen et al. (2008) developed the first regional maximum temperature reconstruction for the Pyrenees based on two local tree-ring chronologies sensitive to temperature variations.

Here, simulations of the climate of the last Millennium with the ECHO-G (González-Rouco et al., 2009) over the Pyrenees region are considered. Additionally, two high resolution regional paleoclimate simulations conducted with the mesoscale model MM5 driven by boundary conditions obtained from the ECHO-G simulations (Gómez-Navarro et al., 2011a, b) are available for the Iberian Peninsula. Hence, for the Pyrenees mountain system, networks of palaeoclimate proxy data (tree-rings) as well as global and regional scale climate simulations are available for inter-comparison.

In the first part of this study we test different methods to construct the tree-ring based climate reconstructions, considering the most usual approaches for the standardization of the individual series, for the development of the regional chronology and for the calibration-reconstruction technique applied. We also compare these resulting reconstruction variants of the Pyrenees temperatures with modified version of the already existing maximum temperature reconstruction based on tree-ring (Büntgen et

[Title Page](#)

[Abstract](#)

[Introduction](#)

[Conclusions](#)

[References](#)

[Tables](#)

[Figures](#)

[◀](#)

[▶](#)

[◀](#)

[▶](#)

[Back](#)

[Close](#)

[Full Screen / Esc](#)

[Printer-friendly Version](#)

[Interactive Discussion](#)



al., 2008), adapted to mean temperatures that will be developed in the present study. The specific aim is to obtain not only a new reconstruction of past temperatures in the Pyrenees, but also an evaluation of the uncertainties related to the methodological variants employed. In the second part of the study, we compare the climate variability reconstructed from the tree-ring records with that simulated by a GCM and a RCM over the Pyrenees area, since this represents an opportunity to evaluate the realism of model simulations in reproducing available evidences of past climate variability.

2 Methods

A dataset of 22 maximum density chronologies (MXD) covering the Pyrenees area was available for the present study, including the two chronologies previously used to develop the first tree-ring based regional reconstruction of past maximum temperatures at the Pyrenees (Büntgen et al., 2008) and additional data published in Büntgen et al. (2010). Compared to this previous maximum temperature reconstruction, the new data set covers a wider area and uses a larger replication, not only in most recent centuries, but also in the earliest part of the period (1260–1350 AD).

The location, elevation and tree species at each site are indicated in Fig. 1. The species sampled were *Pinus uncinata* Ramond ex DC. in Lam. et DC., a shade-intolerant and long-lived conifer growing under temperate subalpine climate conditions and dominating at elevations above 1800 m a.s.l., and *Abies alba* Mill. usually growing at humid sites on north facing, shady slopes and at elevations above 1200 m a.s.l. (Macias et al., 2006).

The 22 MXD chronologies comprise 804 individual tree-ring series from the Pyrenees and nearby mountain areas. As described in Büntgen et al. (2008, 2010), to obtain the MXD measurements from tree-rings, all cores were sanded and visually cross-dated following dendrochronological procedures described by Stokes and Smiley (1968). The accuracy of the visual cross-dating and measurements were verified using the computer program COFECHA (Holmes, 1983). For the

[Title Page](#)[Abstract](#)[Introduction](#)[Conclusions](#)[References](#)[Tables](#)[Figures](#)[|◀](#)[▶|](#)[◀](#)[▶](#)[Back](#)[Close](#)[Full Screen / Esc](#)[Printer-friendly Version](#)[Interactive Discussion](#)

density measurements, lathes perpendicular to the wood fibres were extracted from 804 cores and analysed following X-ray microdensitometric techniques developed by Polge (1965). The output is a density profile of points taken at 0.01 mm intervals in radial direction across each ring. The maximum density along this direction was estimated for each year.
5

2.1 Site chronologies

MXD chronologies for each of the 22 sites were constructed. Density series were processed according to standard dendrochronological techniques (Cook and Kairiukstis, 1990) and individual series were standardized to remove age-trends in the mean by fitting a stiff function which not only emphasizes inter-annual variations but also preserves multi-decadal scale variations in the final chronology (Cook et al., 1995). To assess the uncertainty caused by the application of different standardizations, the individual series underwent different standardization procedures with ARSTAN (Cook and Holmes, 1986). Two detrending techniques were used to remove age trends in the individual series: Regional Curve Standardization (Esper et al., 2003) and a 300-yr cubic smoothing spline with a 50 % frequency-response cut-off. In addition to these two detrending techniques a power transformation (PT) for the stabilization of the variance in the individual series was alternately conducted (Cook and Peters, 1997). Although raw MXD series are assumed to be homoscedastic, we preferred to adopt a conservative position because we do not know the nature of the 804 individual MXD raw series for certain, and the existence of trends in the variance in the series cannot be surely rejected. Thus, a set of four different standardization procedures was applied: (1) Regional Curve standardization (Esper et al., 2003) (RCS) (2) Regional Curve standardization preceded by PT (RCSPT) (3) 300-yr cubic smoothing spline with a 50 % frequency-response cut-off (300 sp) and (4) 300-yr cubic smoothing spline with a 50 % frequency-response cut-off preceded by PT (300 spPT). Finally, for each site, chronologies were constructed by using a bi-weight robust mean which reduces the possible bias caused by extreme values. The final length of the chronologies was
10
15
20
25

[Title Page](#)[Abstract](#)[Introduction](#)[Conclusions](#)[References](#)[Tables](#)[Figures](#)[◀](#)[▶](#)[◀](#)[▶](#)[Back](#)[Close](#)[Full Screen / Esc](#)[Printer-friendly Version](#)[Interactive Discussion](#)

established by truncating the final chronologies when less than 5 contributing samples were available, leading to a maximum reliable time-span of 1260–2005 (Fig. 2).

2.2 Regional Pyrenees chronologies

The 804 individual tree rings MXD series corresponding to the 22 individual MXD site chronologies were standardized and aggregated into regional chronologies using three different approaches: (1) computing a simple arithmetic average of the 22 individual MXD chronologies (RCS_mean, RCSPT_mean, 300 sp_mean, 300 spPT_mean) (2) computing a single chronology including all 804 individual series in one run (RCS_chrono, RCSPT_chrono, 300 sp_chrono, 300 spPT_chrono) and (3) conducting Principal Component Analyses, computed separately for each time segment with a constant number of MXD chronologies to produce nested PCA regional chronologies (PCs_RCS; PCs_RCSPT; PCs_300 sp; PCs_300 spPT). In total, 12 regional chronologies were developed for the Pyrenees region.

Due to the different time-span covered by the 22 chronologies (Fig. 2), a total number of 25 PCA were run for each of the four standardization methods (RCS, RCSPT, 300 sp and 300 spPT) in order to obtain the corresponding scores of the principal components (PCs) in to the time segments. In addition, the spatial loadings, sometimes denoted as Empirical Orthogonal Functions (EOF's) were also analyzed to assess the similarities and differences of their spatial patterns among the four standardization methods. For the EOF's maps we use the loading corresponding to the PCA5 (time span 1928–1977), which includes all 22 MXD chronologies.

Simple correlations were used to assess the climate information contained in the regional chronologies. In mountainous regions as the Pyrenees, temperature series have shown stronger inter-site relationships between distant sites than precipitation data, which display stronger variability at local spatial scales (Agusti-Panareda et al., 2000; Macias et al., 2006; Büntgen et al., 2008, 2010). Temperature is known to be the dominant climate factor controlling tree-growth at the Pyrenees high elevation sites (Macias et al., 2006; Büntgen et al., 2008, 2010). A regional record consisting of the

CPD

7, 3919–3957, 2011

Cross-comparison at the Pyrenees

I. Dorado Liñán et al.

[Title Page](#)

[Abstract](#)

[Introduction](#)

[Conclusions](#)

[References](#)

[Tables](#)

[Figures](#)

◀

▶

◀

▶

[Back](#)

[Close](#)

[Full Screen / Esc](#)

[Printer-friendly Version](#)

[Interactive Discussion](#)



data from six stations: Pamplona, San Sebastián, Zaragoza, Barcelona, Burgos and Huesca (Brunet et al., 2007, 2010) was available as a representative homogenized and high-quality temperature record of the area for the last 100 yr. All regional chronologies, together with the leading principal component PC1 of the PCA, were correlated with instrumental regional temperature averages from Brunet et al. (2007, 2010) at monthly and seasonal time scales. May-to-September mean temperature was identified as the most influencing season for tree growth.

2.3 Pyrenees reconstructions

Pyrenees regional reconstructions were carried out using both scaling and regression methods (Esper et al., 2005b) applied to the different regional chronologies developed. Thus, from the collection of 12 regional MXD chronologies built by means of the three different methodological approaches detailed above, 24 regional reconstructions were developed: 12 using scaling and 12 using regression techniques (Table 1). Calibration/verification tests against the overlapping May-to-September regional instrumental temperature record were performed in split periods (Snee, 1977). The tree-ring model was calibrated on the first half of the instrumental temperature record (1900–1952) and validated on the second half (1953–2005), and vice-versa. Quality control statistics such as the coefficient of determination (r^2) Pearson's correlation coefficient between observed and predicted values ($r_{\text{obs-pred}}$) and the Reduction of Error (RE; Cook et al., 1994) were calculated to test the validity of the reconstructions derived from both methodologies. Reconstruction uncertainties related to the differences of the precursor chronologies and the calibration models used for reconstruction were assessed.

Additionally, the original chronology of Büntgen et al. (2008) (PYR), used to develop the regional maximum temperature reconstruction for the Pyrenees, was calibrated against May–September mean temperatures to build a reconstruction called “mPYR”, fully comparable to the newly developed set of regional mean temperature reconstructions.

[Title Page](#)[Abstract](#)[Introduction](#)[Conclusions](#)[References](#)[Tables](#)[Figures](#)[◀](#)[▶](#)[◀](#)[▶](#)[Back](#)[Close](#)[Full Screen / Esc](#)[Printer-friendly Version](#)[Interactive Discussion](#)

The resulting temperature reconstructions were compared with climate simulations performed with global and regional climate models spanning the last Millennium in the target region.

2.4 Model simulations

- 5 The global GCM simulations used here were produced with the ECHO-G (Legutke and Voss, 1999) climate model, consisting of the the ECHAM4 atmospheric component and the HOPE-G ocean model. ECHAM4 is used with a 730 horizontal resolution (ca. 3.75° lat \times lon) and HOPE-G with a horizontal resolution of approx. 2.8° lat \times lon, with a finer resolution in the tropics increasing towards the Equator where it reaches a
10 minimum meridional grid point separation of 0.5° . The model is run using flux adjustments to avoid climate drift. This work makes use of two existing simulations with this model (Erik1 and Erik2) produced by driving the model with estimations of the evolution of some natural and anthropogenic forcings during the last millennium. The external
15 forcings include estimations of changes in solar irradiance, the parameterized effect of stratospheric volcanic aerosols and concentrations of greenhouse gases (CO_2 , CH_4 and N_2O). Both simulations were produced starting from different initial conditions and driven by identical forcings from year 1000 AD onwards. For a description of the simulations and the used external forcings as well as model details, the reader is referred to Zorita et al. (2005) and González-Rouco et al. (2006, 2009).

- 20 The regional climate model simulations used herein were produced with a climate version of the Fifth-generation Pennsylvania-State University-national Center for Atmospheric Research Mesoscale Model (Dudhia, 1993, Grell et al., 1994). The model domain is double nested with resolutions of 90 km and 30 km, respectively. The high resolution domain covers the area of the Iberian Peninsula. Two 1000 yr long simulations
25 were run. Each simulation (Erik1-MM5 and Erik2-MM5) was produced by driving the MM5 model with boundary conditions obtained from the ECHO-G Erik1 and Erik2 runs, respectively. The boundary conditions are introduced into the outer domain of the MM5 model through a blending area of five grid points at the boundaries. Specifications

Title Page	
Abstract	Introduction
Conclusions	References
Tables	Figures
◀	▶
◀	▶
Back	Close
Full Screen / Esc	

Printer-friendly Version
Interactive Discussion



3 Results

3.1 Regional Pyrenees MXD chronologies and climate signal

- 5 The PCA performed on the set of MXD chronologies to be used in developing regional reconstructions based on nested PCs, reveals that the first principal component (PC1) is dominant and captures on average 60 % of the variance (Fig. 3). The high percentage of explained variance by PC1 shows slight variations across the different PCA runs, displaying higher percentages of explained variance for PCA containing a
10 smaller number of MXD chronologies (PCA1, PCA2, and from PCA20 to PCA24). The leading PC derived from chronologies standardized with 300 sp and 300 spPT, rather than with RCS or RCSPT, also explains slightly more common variance, although the difference is very small. The first Empirical Orthogonal Function (EOF) describes a coherent spatial pattern of the signal regardless of the standardization method used
15 (Fig. 4). The individual points (MXD chronologies) present the same sign and similar magnitude in the maps of the first EOF for each of the four standardization methods. This suggests that spatially coherent modes of tree-ring variation exist, which may reflect regional-scale modes of climate parameters driving tree growth. The second and subsequent PCA modes, which are similar regardless of the standardization method
20 used, become less coherent spatially and seasonally, with sign and magnitude of the relationship, occasionally differing between individual points likely in response to local or site influences.

The leading mode (PC1) shows high correlations with the seasonal May-to-September temperature and has positive loadings across all the Pyrenees sites. The highest correlations with climate are for the PCA that includes the highest number of MXD chronologies (i.e. PCA4 and PCA5) and decreasing with decreasing number of
25

Title Page	
Abstract	Introduction
Conclusions	References
Tables	Figures
◀	▶
◀	▶
Back	Close
Full Screen / Esc	

Printer-friendly Version
Interactive Discussion



series. The small differences observed in the variance captured by PC1 among the different standardization methods have not a significant effect on the correlation between PC1 with May-to-September-temperature (T_{05-09}) (Fig. 5). The coefficients among the different standardization methods are almost identical. In summary, the mean correlation of PC1 with T_{05-09} is 0.64, being slightly higher for the standardization method RCS and RCSPT ($r = 0.65$) than for 300 sp and 300 spPT ($r = 0.63$).

The regional chronologies computed as arithmetic means of the 22 MXD site chronologies (*mean*) display generally higher correlations with T_{05-09} when the standardization methods RCS and RCSPT (RCS_mean and RCSPT_mean respectively) were used rather than 300 sp and 300 spPT (300 sp_mean and 300 sp_mean respectively) (Fig. 5). In comparison to the dominant mode of PCA, only the PC1 of PCA4 and PCA5 display larger correlation coefficients than the RCS_mean and RCSPT_mean. In contrast, among regional series computed as single chrononologies (*chrono*), RCS_chrono and RCSPT_chrono overall display the lowest correlations with T_{05-09} (below 0.4), while 300 sp_chrono and 300 spPT_chrono show coefficients of a similar order of magnitude as those displayed by the PCs.

3.2 May-to-September regional reconstruction: scaling and regression

A total of 24 regional reconstructions for the Pyrenees were developed using both scaling and regression techniques applied to each of the 12 regional chronologies developed. The correlations between the reconstructions based on nested PCs and the instrumental T_{05-09} record are high for both high and low-frequency variations (Table 1). In contrast, correlations for reconstructions from the group chrono are low and they reveal diverging low-frequency information when using RCS and RCSPT as standardization methods (RCS_chrono_R, RCSPT_chrono_R, RCS_chrono_S, RCSPT_chrono_S). Reconstructions based on *mean* regional chronologies display high correlations with the instrumental T_{05-09} , however, slightly lower in the low frequency domain compared to the reconstructions based on nested PCs, similarly as the mPYR.

[Title Page](#)[Abstract](#)[Introduction](#)[Conclusions](#)[References](#)[Tables](#)[Figures](#)[|◀](#)[▶|](#)[Back](#)[Close](#)[Full Screen / Esc](#)[Printer-friendly Version](#)[Interactive Discussion](#)

Cross-comparison at the Pyrenees

I. Dorado Liñán et al.

The calibration-verification test conducted against the target $T05\text{--}09$ in two periods (1900–1953; 1953–2005) generally shows a coherent relationship between observed and predicted values for the 24 regional reconstructions; however, large differences in the reduction of error statistic (RE) appear (Table 1). Regional chronologies based on nested PCs display high correlation coefficients in the two calibration periods, both regression-calibrated ($r_{1900\text{--}1952} = 0.81$ and $r_{1953\text{--}2005} = 0.75$ on average) and scaling-calibrated ($r_{1900\text{--}1952} = 0.73$ and $r_{1953\text{--}2005} = 0.80$ on average). Similarly, REs are also high for the two verifications. On the contrary, even though correlation values are fairly high for the two periods, RE values decline to large negative values when the reconstructed values are obtained by linear regression of single regional chronologies, especially reconstructions from the group *chrono*. Single regional chronologies computed as means display higher RE values when the reconstruction is performed using scaling than regression (RCS_mean_S, RCSPT_mean_S, 300 sp_mean_S, 300 spPT_mean_S). The set of reconstructions based on RCS_chrono and RCSPT_chrono displays RE values of below 0 regardless of the technique used for reconstructing.

The temperature reconstructions for the months May to September ($T05\text{--}09$) span the period from 1265 AD to 2005 AD. From the entire time span, the below-average estimation of the mean May-to-September temperatures by some of the regional reconstructions (RCSPT_chrono_S, RCS_chrono_S, RCSPT_chrono_R and RCS_chrono_R) starts at the beginning of the reconstruction in 1265 and lasts until around 1850 (Fig. 6). mPYR also displays a similar trend but less pronounced than for RCS_chrono_S and RCSPT_chrono_S. Despite this difference regarding the trends, all reconstructions display similar intermediate to low frequency variations, which are, however, less visible in the case of RCSPT_chrono_R and RCS_chrono_R due to their reduced variations amplitude. Periods with persistent climate anomalies such as the Medieval Climate Anomaly (MCA) and the Little Ice Age (LIA) are not pronounced in the set of reconstructions. However, inter-decadal variations clearly register the cold periods coincident with solar minima as those of Dalton (1800–1830 AD), Maunder (1680–1715), Spörer (1480–1520) and Wolf (1340–1380). In addition, a minimum in the modern age

[Title Page](#)
[Abstract](#) [Introduction](#)
[Conclusions](#) [References](#)
[Tables](#) [Figures](#)

[◀](#) [▶](#)
[◀](#) [▶](#)
[Back](#) [Close](#)
[Full Screen / Esc](#)

[Printer-friendly Version](#)
[Interactive Discussion](#)



[Title Page](#)[Abstract](#)[Introduction](#)[Conclusions](#)[References](#)[Tables](#)[Figures](#)[◀](#)[▶](#)[◀](#)[▶](#)[Back](#)[Close](#)[Full Screen / Esc](#)[Printer-friendly Version](#)[Interactive Discussion](#)

between 1950 AD and 1980 AD is shown by all 25 reconstructions including the mPYR. On the other hand, conspicuous maxima also appear during 1300–1330, 1360–1460 and 1710–1740.

3.3 Cross-comparison of model simulation and proxy based climate reconstructions

Simulated May-to-September temperatures show a good agreement with the instrumental record for the first part of the 20th century (Fig. 7a). However, from 1940 onwards the discrepancies arise at the inter-annual time scale, that is, the simulations display peak temperatures which are in contrast to the instrumental record (e.g. between 70 s and 80 s). On the inter-decadal scale, the two global (Erik1 and Erik2) and the regional MM5-Erik2 simulations display a marked positive trend for the entire calibration period in disagreement with the instrumental series. Indeed, the observed instrumental temperatures display a positive trend until 1960 and then a minimum until 1990. This negative temperature trend in the latest part of the 20th century is only reproduced by the regional simulation MM5-Erik1.

Global and regional simulations indicate large inter-decadal changes that are in agreement with those displayed by the collection of May-to-September temperature reconstructions based on MXD from the Pyrenees (Fig. 7b). A high synchrony is found among the simulations and the tree-ring based reconstructions in periods with large negative temperature anomalies observed at the end of the 18th century, during the Dalton and Spörer solar minima, and during periods of positive anomalies as well, e.g. during the middle of the 15th century, middle to end of the 16th century and during the middle of the 18th century. Some simulations lack pronounced negative periods such as the Late Maunder solar minimum which are present in the reconstructions. The simulations Erik1 and MM5-Erik1 display identical periods of negative anomalies corresponding to the Maunder solar minimum, in agreement with the negative anomalies displayed by the set of reconstructions. In the simulations Erik2 and

Cross-comparison at the Pyrenees

I. Dorado Liñán et al.

[Title Page](#)[Abstract](#)[Introduction](#)[Conclusions](#)[References](#)[Tables](#)[Figures](#)[|◀](#)[▶|](#)[◀](#)[▶](#)[Back](#)[Close](#)[Full Screen / Esc](#)[Printer-friendly Version](#)[Interactive Discussion](#)

the pre-industrial period or including the 20th century. Only the reconstructions RC-SPT_chrono_R, RCS_chrono_R, RCSPT_chrono_S and RCS_chrono_S (Fig. 7c) show increased amplitudes when considering the 20th century. Similarly, at inter-decadal timescales, the reconstructions range from the largest amplitude of RCSPT_mean_S

5 (from -2.49 to 0.59°C) to the tiniest of PCs_300_sp_R (from -0.32 to 0.39°C). When considering only the pre-industrial period, changes on the amplitude of variations at inter-decadal scales in the reconstructions do not differ much from the amplitudes considering the whole period.

Generally, the maximum values displayed by the reconstructions are below those
10 showed by the model simulations, regardless of the consideration of the 20th for the calculation. If only considering pre-industrial annual temperature variations (1265–1900) to define the amplitude, the reconstructions based on nested PCs and scaled (PCs_RCS_S; PCs_RCSPT_S; PCs_300_spPT_S; PCs_300_spPT_S) are the ones displaying amplitudes similar to those exhibited by the simulations. However,
15 at inter-decadal timescales, the amplitudes showed by PCs_RCS_S, PCs_RCSPT_S, PCs_300_spPT_S and PCs_300_spPT_S (from -0.97 to 0.28°C ; from -1 to 0.37°C ; from -0.66 to 0.38°C and from -0.81 to 0.4°C , respectively) are smaller than those exhibited by the model simulations, especially MM5-Erik1.

4 Discussion

20 How the individual chronologies should be standardized to remove local influences preserving at the same time as much climate information as possible, is a key challenge in dendroclimatology. Increased efficiency in preserving low-frequency climate information in tree-ring records will improve the usage of such proxy data for climate reconstructions and model validation. The regional chronology standardization (RCS;
25 Esper et al., 2003) does not preserve decadal or annual frequencies with better efficiency than other techniques (Bunn et al., 2004) but it is assumed to retain more low frequency variability than more traditional standardization techniques (i.e. 300-yr spline).

CPD

7, 3919–3957, 2011

Cross-comparison at the Pyrenees

I. Dorado Liñán et al.

[Title Page](#)

[Abstract](#)

[Introduction](#)

[Conclusions](#)

[References](#)

[Tables](#)

[Figures](#)

◀

▶

◀

▶

[Back](#)

[Close](#)

[Full Screen / Esc](#)

[Printer-friendly Version](#)

[Interactive Discussion](#)



On the other hand, the proxy-based climate reconstructions need to encode a climate signal which is not locally confined to be suitable for comparison with model outputs, since simulations can only capture main climate features with a spatial scale comparable at least to the spatial resolution of the models. Thus, individual or site chronologies
5 should ideally be aggregated into one regional chronology to capture a regional rather than a local climate signal. So far, the construction of regional reconstructions from a set of several individual chronologies (from the same and/or different variables) have been achieved by PCA (Peters et al., 1981; Enright et al., 1984; D'Arrigo et al., 1999)
10 arithmetic means (Briffa et al., 2004; Tang et al., 2009) or regional chronologies compiled into a single file including all the individual measurements (Esper et al., 2007; Büntgen et al., 2008).

The standardization technique used have contributed to visible differences among various reconstructions as reported by other authors (Esper et al., 2002, Helama et al., 2004) and our results suggest that these differences may be enhanced when deriving a regional chronology from the individual chronologies. We could not find large differences among regional reconstructions when they were calculated as an average of the 22 MXD site chronologies (*mean*) or when using nested PCs (PCs), regardless of the standardization method applied to the individual chronologies. In this case, the four standardization procedures yielded similar results. The similarity
15 between *mean* and nested PCs regional chronologies comes as no surprise, since, the PCA approach to define a regional chronology is known to produce similar results to those obtained using the arithmetic mean (Peters et al., 1981). Differences due to the standardization arose in the regional reconstructions which were derived from regional chronologies computed as a single chronology including all 804 individual series in one run (the group named *chrono*). Regional chronologies from the group *chrono*, standardized with a 300 yr spline (with or without power transformation: 300 spPT_chrono and 300 sp_chrono, respectively) still produced similar results
20 as those of *mean* and PCs regional chronologies. Differences appeared when calculating the regional chronology *chrono* using RCS (with and without PT: RCSPT_chrono
25

[Title Page](#)[Abstract](#)[Introduction](#)[Conclusions](#)[References](#)[Tables](#)[Figures](#)[|◀](#)[▶|](#)[◀](#)[▶](#)[Back](#)[Close](#)[Full Screen / Esc](#)[Printer-friendly Version](#)[Interactive Discussion](#)

Cross-comparison at the Pyrenees

I. Dorado Liñán et al.

and RCS_chrono, respectively). Correlations between T05–09 and RCS_chrono and RCSPT_chrono are consistently lower compared to the correlations displayed by other regional chronologies, pointing to a less preserved climate signal in RCS_chrono and RCSPT_chrono. Furthermore, the resulting reconstructions disagree in some aspects
5 with any other newly developed reconstruction, e.g. concerning a pronounced positive trend spanning the entire series lengths (RCSPT_chrono_S and RCS_chrono_S), and the extremely reduced amplitude of past climate variations (RCSPT_chrono_R and RCS_chrono_R). In contrast, the two regional chronologies derived of a similar procedure but different standardization (300 sp_chrono and 300 spPT_chrono) display high
10 correlations with temperature and the reconstructions based on these two chronologies are similar to the ones derived from the regional chronologies *mean* and PCs. Therefore, it becomes obvious that the differences stem from the computation of the regional chronology, not only by using a single file containing all the individual measurements but also from the application of the RCS as the standardization method.

15 RCS requires sampling loads structured in age classes with similar replication (Esper et al., 2002), which limits its application in practice. Although it has been found that RCS does not seem to be so sensitive to some of these requirements as initially thought (i.e. pith off-set; Esper et al., 2003, 2009), it seems that sample depth and age structure have strong effects on the resulting chronology (Esper et al., 2003; Bunn
20 et al., 2004; Briffa and Melvin, 2008). The set of samples from the Pyrenees does not fulfil the RCS requirements: the sample depth diagram shows an extremely high number of samples concentrated in the most recent period (from 1800 to 2005 AD, approximately), whereas the replication in the rest of the period (from 1265 to 1800 AD) is much lower. Such anomalously high and low replications can introduce a bias into
25 the final chronology (Cook and Peters, 1997; Esper et al., 2003; Helama et al., 2004) and therefore in the resulting reconstruction. Thus, based in the sample distribution and the low calibration statistics, it seems likely that the trend of RCSPT_chrono_S and RCS_chrono_S may be an artefact due to a suboptimal data set used for the regional chronology constructed using RCS. Such a trend was removed in the case of

[Title Page](#)[Abstract](#)[Introduction](#)[Conclusions](#)[References](#)[Tables](#)[Figures](#)[|◀](#)[▶|](#)[◀](#)[▶](#)[Back](#)[Close](#)[Full Screen / Esc](#)[Printer-friendly Version](#)[Interactive Discussion](#)

Cross-comparison at the Pyrenees

I. Dorado Liñán et al.

[Title Page](#)[Abstract](#)[Introduction](#)[Conclusions](#)[References](#)[Tables](#)[Figures](#)[|◀](#)[▶|](#)[◀](#)[▶](#)[Back](#)[Close](#)[Full Screen / Esc](#)[Printer-friendly Version](#)[Interactive Discussion](#)

instrumental measurements and proxy estimates has been previously described and the possible causes discussed (Frank et al., 2007). The tree-ring data from the Pyrenees display a strong and stable relationship with the climate variable and, therefore, a loss of tree sensitivity to climate seems unlikely (“divergence problem”; Briffa et al., 5 1998, D’Arrigo et al., 2008). Thus, this mismatch may be due to the effect of the standardization methods on the low-frequency climate information encoded in tree-ring series (Cook et al., 1995; Esper et al., 2002) or alternatively related to the instrumental data used for calibration (Frank et al., 2007; Esper et al., 2005b, 2010). The selected 10 instrumental data for the Pyrenees and the homogenization and adjustments applied to these data also have a determinant effect on the resulting proxy-based reconstructions (Frank et al., 2007). In our case, no clear conclusion can be drawn without further specific work directed to answer this particular question.

The comparison between the output of the model simulations and the range established by the different reconstructions shows that the agreement between reconstructed and simulated May-to-September temperatures at the Pyrenees is good, especially at intermediate to low frequencies. At multi-decadal timescales, the different 15 series exhibit synchronized variability with a similar behaviour, e.g. a warmer century from 1300 AD to 1400 AD, a colder period between 1600–1800 AD (little ice age, LIA), the solar minima and the modern warming. Thus, the external forcings applied to the model matches the timing of the main past periods of anomalous temperatures in 20 the Pyrenees region. Actually, the spread among the four simulated temperatures is mostly within the range estimated from the different standardization and reconstruction methods applied over the last 750 yr. Similar results comparing simulations and proxy based temperature reconstructions have been described by D’Arrigo et al. (1999) for the Northern Hemisphere and by Tan et al. (2009) for China.

Differences between reconstructions and model simulations usually arise in regard to the duration and magnitude of warming or cooling events of particular climatic episodes. Erik1 seems to stay in better agreement with the variability displayed by the proxy-based reconstructions. In addition to the agreement concerning the maxima

Cross-comparison at the Pyrenees

I. Dorado Liñán et al.

[Title Page](#)[Abstract](#)[Introduction](#)[Conclusions](#)[References](#)[Tables](#)[Figures](#)[|◀](#)[▶|](#)[◀](#)[▶](#)[Back](#)[Close](#)[Full Screen / Esc](#)[Printer-friendly Version](#)[Interactive Discussion](#)

and minima reproduced by all four simulations, Erik1 and MM5-Erik1 also match in the warm and cold periods which occurred in the 15th to 16th century (including the Maunder solar minimum). However, those episodes were not captured by Erik2.

Model simulations also show some clear discrepancies in comparison to the tree-ring based reconstructions. The most relevant is the positive trend from 1850 to present displayed by the simulations but not reproduced by the reconstructions. We already know that reconstructions may underestimate the climate variations but since the model runs incorporate both natural and anthropogenic forcings, it is difficult to distinguish the effect of the individual forcings in the resulting simulation and especially in the resulting trend. Thus, it is difficult to know whether the observed difference between simulations and reconstructions is due to an underestimation of the proxy-based reconstructions or by an overestimation of the models.

At higher frequencies, i.e. decadal time scales, the agreement between model simulations and reconstructions is lower because the climate variability at this time scales is mostly internal and not driven by the external forcing (Zorita et al., 2007; Gómez-Navarro et al., 2011b). For instance, a warm episode with the maximum around AD 1730 displayed by the Pyrenees reconstructions is not reproduced by any of the four simulations and does not match any maximum of the external forcing. This maximum in temperature has been described for other European temperature reconstruction (Leijonhufvud et al., 2010; Zorita et al., 2010), which points to a regional to hemispheric-scale maximum generated by internal climate dynamics. Therefore, this particular warm episode may not necessarily appear in the simulations due to the possible shortcomings of models in regard to model internal climate dynamics.

The 20th century is highlighted as an interesting period for evaluating the skill of both proxy based reconstructions and model simulations to replicate climate variations. The instrumental data used for the Pyrenees describe a pronounced cooling from 1950 until approximately 1980, which is visible in the reconstructions but is not found in the simulations. Moreover, this cooling period does not agree with the increasing warming trend replicated by simulations for the second part of the 20th century. Actually,

Cross-comparison at the Pyrenees

I. Dorado Liñán et al.

[Title Page](#)[Abstract](#)[Introduction](#)[Conclusions](#)[References](#)[Tables](#)[Figures](#)[|◀](#)[▶|](#)[◀](#)[▶](#)[Back](#)[Close](#)[Full Screen / Esc](#)[Printer-friendly Version](#)[Interactive Discussion](#)

Cross-comparison at the Pyrenees

I. Dorado Liñán et al.

[Title Page](#)[Abstract](#)[Introduction](#)[Conclusions](#)[References](#)[Tables](#)[Figures](#)[|◀](#)[▶|](#)[◀](#)[▶](#)[Back](#)[Close](#)[Full Screen / Esc](#)[Printer-friendly Version](#)[Interactive Discussion](#)

than in reconstructions if we consider the whole common period (1265–1990). However, if the 20th century is not considered, the amplitude of the annual temperature variations are usually wider in the tree-ring based reconstructions performed with scaling than in model simulations. Furthermore, reconstructions performing better calibrations with the instrumental record (PCs_RCS_S; PCs_RCSPT_S; PCs_300 spPT_S; PCs_300 spPT_S) are also displaying annual amplitudes closer to those of the model outputs.

5 Conclusions

Similarities between the inter-decadal temperature variations obtained with all standardization methods indicate the good performance of all standardization procedures for retaining inter-annual to inter-decadal climate information. However, when the regionally representative tree-ring series are built as a single chronology (concentrating all single measurements into one file) and standardized with the RCS method, odd results may be obtained if the requirements of sample replication and age categorization are not fulfilled for the RCS method. Overall, nested PCs have demonstrated to be the most appropriate approach to build a regional chronology based on a set of local chronologies, regardless of the standardization procedure used for the individual site chronologies. Additionally, no large differences were found between reconstruction techniques (scaling and regression) when using chronologies based on nested PCs. Thus, the quality of the final reconstruction seems to depend more on the standardization performed and the method applied to construct the regional chronology, rather than on the reconstruction method employed.

We provide a set of newly developed May-to-September mean temperature reconstructions for the Pyrenees which represent an improvement in comparison to the reconstruction by Büntgen et al. (2008), although our reconstructions still do not perfectly match the low-frequency variations of the instrumental record.

[Title Page](#)[Abstract](#)[Introduction](#)[Conclusions](#)[References](#)[Tables](#)[Figures](#)[|◀](#)[▶|](#)[◀](#)[▶](#)[Back](#)[Close](#)[Full Screen / Esc](#)[Printer-friendly Version](#)[Interactive Discussion](#)

Cross-comparison at the Pyrenees

I. Dorado Liñán et al.

[Title Page](#)[Abstract](#)[Introduction](#)[Conclusions](#)[References](#)[Tables](#)[Figures](#)[|◀](#)[▶|](#)[◀](#)[▶](#)[Back](#)[Close](#)[Full Screen / Esc](#)[Printer-friendly Version](#)[Interactive Discussion](#)

Nevertheless, the good agreements on inter-decadal scales between tree-ring based reconstructions and global and regional model simulations points to solar variability combined with volcanic activity as the main factors driving summer temperature variations over the last millennium at the Pyrenees. Since we have developed regional

reconstructions, it is difficult to conclude whether the more realistic topography and land use categories of the regional model would yield a more accurate replication of temperature variations at local scales, but it does seem to yield larger amplitude of temperature variations compared to the global models.

An important point is that the instrumental and reconstructed temperature series do not agree with the increasing trend displayed by the simulations for the 20th century. This trend is most probably due to the greenhouse gas forcing over the more recent period but since the model runs incorporate both natural and anthropogenic forcing, it is difficult to distinguish the effect of the individual forcings in the resulting simulation and especially in the resulting trend. In addition, cooling factors such as aerosols and vegetation changes are not included as external forcings in the simulations and their contributions to the changes in the surface temperatures are still unclear.

Acknowledgements. We thank Björn Günther and Daniel Nievergelt for performing the density measurements and Pedro Ángel Jiménez Muñoz for providing the data for the map. This research was funded by MILLENNIUM (017008-2).

References

Agustí-Panareda, A., Thompson, R., and Livingstone, D. M.: Reconstructing temperature variations at high elevation lake sites in Europe during the instrumental period, Verh. Int. Ver. Limn., 27, 479–483, 2000.

Briffa K. R. and Melvin, T. M.: A closer look at Regional Curve Standardisation of tree-ring records: justification of the need, a warning of some pitfalls, and suggested improvements in its application, in: Dendroclimatology: Progress and Prospects, edited by: Hughes, M. K., Diaz, H.F., Swetnam, T. W., Springer Verlag, 2008.

Cross-comparison at the Pyrenees

I. Dorado Liñán et al.

[Title Page](#)

[Abstract](#)

[Introduction](#)

[Conclusions](#)

[References](#)

[Tables](#)

[Figures](#)

◀

▶

◀

▶

[Back](#)

[Close](#)

[Full Screen / Esc](#)

[Printer-friendly Version](#)

[Interactive Discussion](#)



- Briffa, K. R., Schweingruber, F., Jones, P., and Osborn, T.: Reduced sensitivity of recent tree growth to temperature at high northern latitudes, *Nature*, 391, 678–682, 1998.
- Briffa, K. R., Osborn, T. J., Schweingruber, F. H., Jones, P. D., Shiyatov, S. G., and Vaganov, E. A.: Tree-ring width and density data around the Northern Hemisphere: part 1, local and regional climate signals, *Holocene*, 12, 737–757, 2002.
- Briffa, K. R., Osborn, T. J., and Schweingruber, F. H.: Large-scale temperature inferences from tree rings: a review, *Global Planet. Change*, 40, 11–26, 2004.
- Brunet, M., Jones, P. D., Sigro, J., Saladie, O., Aguilar, E., Moberg, A., Della-Marta, P. M., Lister, D., Walther, A., and Lopez, D.: Temporal and spatial temperature variability and change over Spain during 1850–2005, *J. Geophys. Res.-Atmos.*, 112, D12117, doi:10.1029/2006JD008249, 2007.
- Brunet, M., Asin, J., Sigró, J., Bañón, M., García, F., Aguilar, E., Palenzuela, J. E., Peterson, T. C., and Jones, P.: The minimization of the screen bias from ancient Western Mediterranean air temperature records: an exploratory statistical analysis, *Int. J. Climatol.*, doi:10.1002/joc.2192, 2010.
- Büntgen, U., Frank, D. C., Nievergelt, D., and Esper, J.: Summer temperature variations in the European Alps, AD 755–2004, *J. Climate*, 19, 5606–5623, 2006.
- Büntgen, U., Frank, D. C., Kaczka, R. J., Verstege, A., Zwijacz-Kozica, T., and Esper, J.: Growth/climate response of a multi-species tree-ring network in the Western Carpathian Tatra Mountains, Poland and Slovakia, *Tree Physiol.*, 27, 689–702, 2007.
- Büntgen, U., Frank, D. C., Grudd, H., and Esper, J.: Long-term summer temperature variations in the Pyrenees, *Clim. Dynam.*, 31, 615–631, 2008.
- Büntgen, U., Frank, D. C., Trouet, V., and Esper, J.: Diverse climate sensitivity of Mediterranean tree-ring width and density, *Trees-Struct. Funct.*, 24, 261–273, 2010.
- Bunn, A. G., Sharac, T. J., and Graumlich, L. J.: Using a simulation model to compare methods of tree-ring detrending and to investigate the detectability of low-frequency signals, *Tree-Ring Res.*, 60, 77–90, 2004.
- Collins, W. D., Rasch, P. J., Eaton, B., Fillmore, D. W., Kiehl, J., Beck, T. C., and Zender, C.: Simulation of Aerosol Distributions and Radiative Forcing for INDOEX: Regional Climate Impacts, *J. Geophys. Res.*, 107, 8028, 2002.
- Cook, E. R. and Holmes, R. L.: Program ARSTAN, Version 1, 72 pp., 1986.
- Cook, E. R. and Kairiukstis, L. A.: Methods of dendrochronology: applications in the environmental sciences. International Institute for Applied Systems Analysis, Boston, MA, USA,

Cross-comparison at the Pyrenees

I. Dorado Liñán et al.

[Title Page](#)[Abstract](#)[Introduction](#)[Conclusions](#)[References](#)[Tables](#)[Figures](#)[◀](#)[▶](#)[◀](#)[▶](#)[Back](#)[Close](#)[Full Screen / Esc](#)[Printer-friendly Version](#)[Interactive Discussion](#)

Kluwer Academic Publishers, 1990.

Cook, E. R. and Peters, K.: Calculating unbiased tree-ring indices for the study of climatic and environmental change, *Holocene*, 7, 361–370, 1997.Cook, E. R., Briffa, K. R., and Jones, P. D.: Spatial regression methods in dendroclimatology: A review and comparison of two techniques, *Int. J. Climatol.*, 14, 379–402, 1994.Cook, E. R., Briffa, K. R., Meko, D. M., Graybill, D. A., and Funkhouser, G.: The segment length curse in long tree-ring chronology development for paleoclimatic studies, *Holocene*, 5, 229–37, 1995.D'Arrigo, R. D., Gordon, C. J., Free, M., and Robock, A.: Northern Hemisphere annual to decadal temperature variability for the past three centuries: Tree-ring and model estimates, *Climatic Change*, 42, 663–675, 1999.D'Arrigo, R., Wilson, R., Liepert, B., and Cherubini, P.: On the 'Divergence Problem' in Northern Forests: A Review of the Tree-Ring Evidence and Possible Causes, *Global Planet. Change*, 60, 289–305, 2008.15 Dudhia, J.: A nonhydrostatic version of the Penn StateNCAR mesoscale model: Validation tests and simulation of an Atlantic cyclone and cold front, *Mon. Weather Rev.*, 121, 1493–1513, 1993.Enright, N. J.: Principal components analysis of tree-ring/climate relationships in white spruce (*Picea glauca*) from Schefferville, Canada, *J. Biogeogr.*, 11, 353–361, 1984.20 Esper, J., Cook, E. R., and Schweingruber, F. H.: Low-frequency signals in long tree-ring chronologies and the reconstruction of past temperature variability, *Science*, 295, 2250–2253, 2002.Esper, J., Cook, E. R., Krusic, P. J., Peters, K., and Schweingruber, F. H.: Tests of the RCS method for preserving low-frequency variability in long tree-ring chronologies, *Tree-Ring Res.*, 59, 81–98, 2003.25 Esper, J., Frank, D. C., and Wilson, R. J. S.: Climate reconstructions: low frequency ambition and high frequency ratification, *EOS*, 85, 113–130, 2004.Esper, J., Wilson, R. J. S., Frank, D. C., Moberg, A., Wanner, H., and Luterbacher, J.: Climate: past ranges and future changes, *Quaternary Sci. Rev.*, 24, 2164–2166, 2005a.30 Esper, J., Frank, D. F., Wilson, R. J. S., and Briffa, K. R.: Effect of scaling and regression on reconstructed temperature amplitude for the past millennium, *Geophys. Res. Lett.*, 32, L07711, doi:10.1029/2004GL021236, 2005b.

Esper, J., Frank, D., Büntgen, U., Verstege, A., Luterbacher, J., and Xoplaki, E.:

Cross-comparison at the Pyrenees

I. Dorado Liñán et al.

- Long-term drought severity variations in Morocco, *Geophys. Res. Lett.*, 34, L17702, doi:10.1029/2007GL030844, 2007.
- Esper, J., Frank, D., Büntgen, U., and Kirdyanov, A.: Influence of pith offset on tree-ring chronology trend, *TRACE* 7, 205–210, 2009.
- 5 Esper, J., Frank, D., Büntgen, U., Verstege, A., Hantemirov, R. M., and Kirdyanov, A.: Trends and uncertainties in Siberian indicators of 20th century warming, *Glob. Change Biol.*, 16, 386–398, 2010.
- Frank, D. C., Büntgen, U., Böhm, R., Maugeri, M., and Esper, J.: Warmer early instrumental measurements versus colder reconstructed temperatures: shooting at a moving target, *Quaternary Sci. Rev.*, 26, 3298–3310, 2007.
- 10 Fritts, H. C.: *Tree Rings and Climate*, Academic Press, New York, 1976.
- Garcia-Ruiz, J. M. and Lasanta, T.: Land use changes in the Spanish Pyrenees, *Mt. Res. Dev.*, 10, 201–214, 1990.
- Gómez-Navarro, J. J., Montávez, J. P., Jerez, S., Jiménez-Guerrero, P., Lorente-Plazas, R., González-Rouco, J. F., and Zorita, E.: A regional climate simulation over the Iberian Peninsula for the last millennium, *Clim. Past*, 7, 451–472, doi:10.5194/cp-7-451-2011, 2011a.
- 15 Gómez-Navarro, J. J., Montávez, J. P., Jiménez-Guerrero, P., Jerez, S., Lorente-Plazas, R., González-Rouco, J. F., and Zorita, E.: Internal and external variability in regional simulations of the Iberian Peninsula climate over the last millennium, *Clim. Past Discuss.*, 7, 2579–2607, doi:10.5194/cpd-7-2579-2011, 2011b.
- 20 González-Rouco, J. F., Beltrami, H., Zorita, E., and von Storch, H.: Simulation and inversion of borehole temperature profiles in surrogate climates: Spatial distribution and surface coupling, *Geophys. Res. Lett.*, 33, L024693, doi:10.1029/2005GL024693, 2006.
- González-Rouco, J. F., Beltrami, H., Zorita, E., and Stevens, M. B.: Borehole climatology: a discussion based on contributions from climate modeling, *Clim. Past*, 5, 97–127, doi:10.5194/cp-5-97-2009, 2009.
- 25 Grell, G. A., Dudhia, J., and Stauger, D. R.: A description of the fifth-generation penn state/ncar mesoscale model (mm5). – Technical Report NCAR/TN-398+STR, National Center for Atmospheric Research, 1994.
- Grudd, H.: Tornetrask tree-ring width and density AD 500–2004: a test of climatic sensitivity and a new 1500 year reconstruction of northern Fennoscandian summers, *Clim. Dynam.*, 31, 843–857, 2008.
- 30 Hansen, J., Sato, M., Nazarenko, L., Ruedy, R., Lacis, A., Koch, D., Tegen, I., Hall, T., Shin-

[Title Page](#)[Abstract](#)[Introduction](#)[Conclusions](#)[References](#)[Tables](#)[Figures](#)[◀](#)[▶](#)[◀](#)[▶](#)[Back](#)[Close](#)[Full Screen / Esc](#)[Printer-friendly Version](#)[Interactive Discussion](#)

- dell, D., Santer, B., Stone, P., Novakov, T., Thomason, L., Wang, R., Wang, Y., Jacob, D., Hollandsworth, S., Bishop, L., Logan, J., Thompson, A., Stolarski, R., Lean, J., Willson, R., Levitus, S., Antonov, J., Rayner, N., Parker, D., and Christy, J.: Climate forcings in Goddard Institute for Space Studies SI2000 simulations, *J. Geophys. Res.*, 107, 4347, doi:10.1029/2001JD001143, 2002.
- Hegerl, G. C., Crowley, T. J., Hyde, W. T., and Frame, D. J.: Climate sensitivity constrained by temperature reconstructions over the past seven centuries, *Nature*, 440, 1029–1032, 2006.
- Helama, S., Lindholm, M., Timonen, M., and Eronen, M.: Detection of climate signal in dendrochronological data analysis: A comparison of tree ring standardization methods, *Theor. Appl. Climatol.*, 79, 239–254, 2004.
- Holmes R. L.: Computer-assisted quality control in tree-ring dating and measurement, *Tree-Ring Bulletin*, 43, 69–78, 1983.
- IPCC: Climate change, fourth assessment report, Cambridge University Press, London, UK, 2007.
- Jansen, E., Overpeck, J., Briffa, K. R., Duplessy, J. C., Masson-Delmontte, V., Olago, D., Otto-Bliesner, B., Peltier, W. R., Rahmstorf, S., Ramesh, R., Raynaud, D., Rind, D., Solomina, O., Villalba, R., and Zhang, D.: Paleoclimate, in: *Climate Change 2007: The Physical Science Basis. Contribution of Working Group I to the Fourth Assessment Report of the Intergovernmental Panel on Climate Change*, edited by: Solomon, S., Qin, D., Manning, M., Chen, Z., Marquis, M., Averyt, K. B., Tignor, M., and Miller, H. L., Cambridge, United Kingdom and New York, NY, USA: Cambridge University Press, 2007.
- Jones, P. D. and Mann, M. E.: Climate over past millennia, *Rev. Geophys.*, 42, RG2002, doi:10.1029/2003RG000143, 2004.
- Jones, P. D., Briffa, K. R., Osborn, T. J., Lough, J. M., van Ommen, T. D., Vinther, B. M., Luterbacher, J., Wahl, E. R., Zwiers, F. W., Mann, M. E., Schmidt, G. A., Ammann, C. M., Buckley, B. M., Cobb, K. M., Esper, J., Goosse, H., Graham, N., Jansen, E., Kiefer, T., Kull, C., Küttel, M., Mosley-Thompson, E., Overpeck, J. T., Riedwyl, N., Schulz, M., Tudhope, A. W., Villalba, R., Wanner, H., Wolff, E., and Xoplaki, E.: High-resolution palaeoclimatology of the last millennium: a review of current status and future prospects, *Holocene*, 19, 3–49, 2009.
- Lasanta, T. and Vicente-Serrano, S. M.: Cambios en la cubierta vegetal en el Pirineo Aragonés en los últimos 50 años, *Pirineos*, 162, 125–154, 2007 (in Spanish).
- Legutke, S. and Voss, R.: The Hamburg Atmosphere-Ocean Coupled Circulation Model ECHO-

[Title Page](#)[Abstract](#)[Introduction](#)[Conclusions](#)[References](#)[Tables](#)[Figures](#)[|◀](#)[▶|](#)[◀](#)[▶](#)[Back](#)[Close](#)[Full Screen / Esc](#)[Printer-friendly Version](#)[Interactive Discussion](#)

Cross-comparison at the Pyrenees

I. Dorado Liñán et al.

[Title Page](#)[Abstract](#)[Introduction](#)[Conclusions](#)[References](#)[Tables](#)[Figures](#)[|◀](#)[▶|](#)[◀](#)[▶](#)[Back](#)[Close](#)[Full Screen / Esc](#)[Printer-friendly Version](#)[Interactive Discussion](#)

2007.

Zorita, E., Moberg, A., Leijonhufvud, L., Wilson, R., Brazdil, R., Dobrovolny, P., Luterbacher, J., Bohm, R., Pfister, C., Glaser, R., Soderberg, J., and González-Rouco, F.: European temperature records of the past five centuries based on documentary information compared to climate simulations, *Climatic Change*, 101, 143–168, 2010.

5

CPD

7, 3919–3957, 2011

Cross-comparison at the Pyrenees

I. Dorado Liñán et al.

[Title Page](#)

[Abstract](#)

[Introduction](#)

[Conclusions](#)

[References](#)

[Tables](#)

[Figures](#)

◀

▶

◀

▶

[Back](#)

[Close](#)

[Full Screen / Esc](#)

[Printer-friendly Version](#)

[Interactive Discussion](#)



Cross-comparison at the Pyrenees

I. Dorado Liñán et al.

Reconstruction technique	regional reconstruction code	Split period					
		<i>r</i>	<i>r_{lf}</i>	<i>r_{1900–1952}</i>	<i>r_{1953–2005}</i>	RE1	RE2
Single regional chronology							
Regression	RCS_mean_R	0.70**	0.45	0.73**	0.81**	0.09	0.42
	RCSPT_mean_R	0.72**	0.49	0.73**	0.82**	0.21	0.43
	300 sp_mean_R	0.60**	0.20	0.73**	0.74**	-0.24	0.12
	300 spPT_mean_R	0.61**	0.22	0.74**	0.74**	-0.29	0.00
	RCS_chrono_R	0.36**	-0.19	0.75**	0.54**	-0.70	-0.80
	RCSPT_chrono_R	0.37**	-0.18	0.74**	0.55**	-0.82	-0.94
	300 sp_chrono_R	0.59**	0.25	0.75**	0.72**	-0.12	-0.37
	300 spPT_chrono_R	0.59**	0.25	0.72**	0.72**	-0.02	-0.43
Scaling	RCS_mean_S	0.71**	0.45	0.73**	0.81**	0.36	0.69
	RCSPT_mean_S	0.72**	0.49	0.73**	0.82**	0.36	0.66
	300 sp_mean_S	0.60**	0.20	0.73**	0.74**	0.36	0.40
	300 spPT_mean_S	0.61**	0.22	0.74**	0.74**	0.28	0.47
	RCS_chrono_S	0.36**	-0.19	0.75**	0.54**	-0.04	-4.20
	RCSPT_chrono_S	0.37**	-0.18	0.75**	0.55**	-0.02	-3.95
	300 sp_chrono_S	0.59**	0.25	0.75**	0.72**	0.22	0.38
	300 spPT_chrono_S	0.59**	0.25	0.72**	0.72**	0.21	0.44
Nested PCs regional chronology							
Regression	PCs_RCS_R	0.73**	0.56	0.81**	0.76**	0.59	0.67
	PCs_RCSPT_R	0.80**	0.58	0.81**	0.84**	0.73	0.68
	PCs_300 sp_R	0.67**	0.43	0.81**	0.70**	0.51	0.65
	PCs_300 spPT_R	0.68**	0.45	0.81**	0.70**	0.51	0.66
Scaling	PCs_RCS_S	0.71**	0.64	0.73**	0.83**	0.65	0.62
	PCs_RCSPT_S	0.72**	0.78	0.73**	0.84**	0.66	0.62
	PCs_300 sp_S	0.66**	0.53	0.73**	0.76**	0.46	0.62
	PCs_300 spPT_S	0.66**	0.55	0.74**	0.77**	0.48	0.61
Modified Büntgen et al. (2008), mPYR		0.62**	0.61	0.57**	0.74**	0.47	-0.85



- [Title Page](#)
- [Abstract](#) [Introduction](#)
- [Conclusions](#) [References](#)
- [Tables](#) [Figures](#)
- [◀](#) [▶](#)
- [◀](#) [▶](#)
- [Back](#) [Close](#)
- [Full Screen / Esc](#)
- [Printer-friendly Version](#)
- [Interactive Discussion](#)

Cross-comparison at the Pyrenees

I. Dorado Liñán et al.

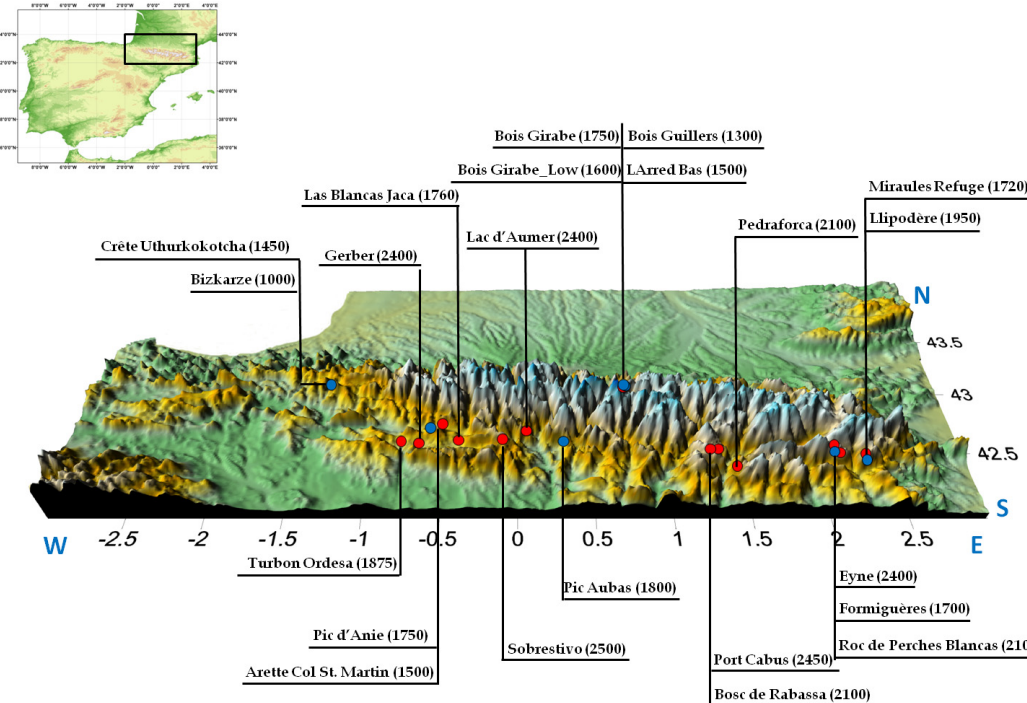


Fig. 1. Location of the 22 MXD chronologies. Close red and blue circles indicate the tree species sampled at each site: *Pinus uncinata* and *Abies alba*, respectively. The elevations (in meters above sea level) are indicated in brackets.

[Title Page](#)

[Abstract](#)

[Introduction](#)

[Conclusions](#)

[References](#)

[Tables](#)

[Figures](#)

[◀](#)

[▶](#)

[◀](#)

[▶](#)

[Back](#)

[Close](#)

[Full Screen / Esc](#)

[Printer-friendly Version](#)

[Interactive Discussion](#)



Cross-comparison at the Pyrenees

I. Dorado Liñán et al.

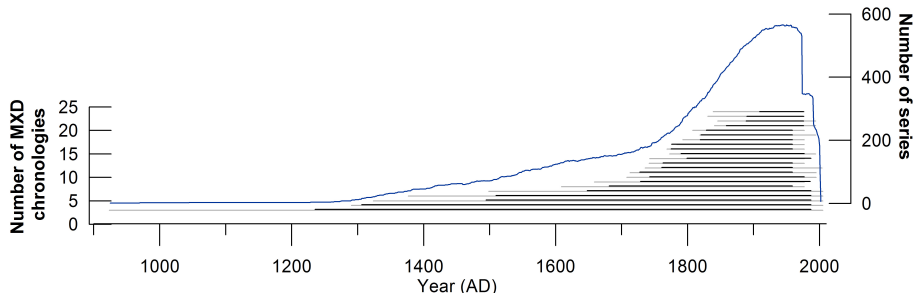
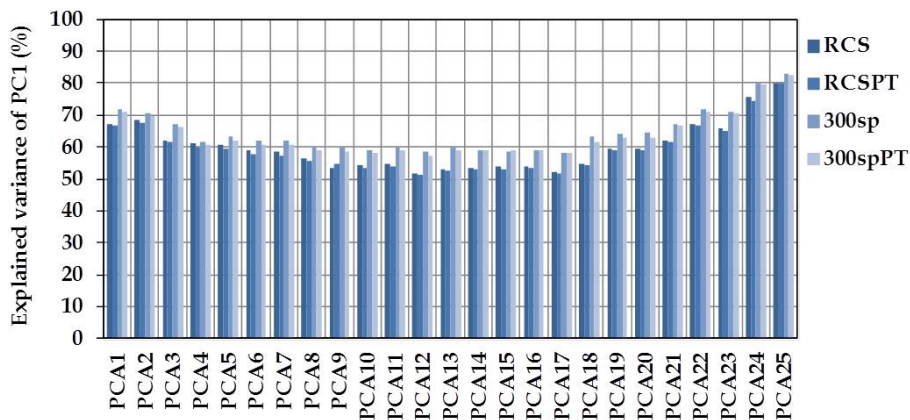


Fig. 2. Total time-span (grey line) and reliable time span (black line) after truncation of the 22 MXD chronologies at >5 series. Blue line represents total number of MXD series.

[Title Page](#)[Abstract](#)[Introduction](#)[Conclusions](#)[References](#)[Tables](#)[Figures](#)[|◀](#)[▶|](#)[◀](#)[▶](#)[Back](#)[Close](#)[Full Screen / Esc](#)[Printer-friendly Version](#)[Interactive Discussion](#)

Cross-comparison at the Pyrenees

I. Dorado Liñán et al.



PCA	time span	PCA	time span	PCA	time span
PCA1	1669-2005	PCA10	1840-1977		
PCA2	1749-2004	PCA11	1839-1977	PCA19	1749-1977
PCA3	1806-1995	PCA12	1819-1977	PCA20	1748-1977
PCA4	1928-1994	PCA13	1810-1977	PCA21	1702-1977
PCA5	1928-1977	PCA14	1794-1977	PCA22	1669-2005
PCA6	1909-1977	PCA15	1795-1977	PCA23	1517-2005
PCA7	1908-1977	PCA16	1783-1977	PCA24	1477-2005
PCA8	1878-1977	PCA17	1781-1977	PCA25	1330-2005
PCA9	1848-1977	PCA18	1763-1977		

Fig. 3. Explained variance of the PC1 for each PCA analysis (1 to 25) and for each standardization method (RCS, RCSPT, 300 sp, 300 spPT). Time span for each PCA are shown in the bottom table.

Cross-comparison at
the Pyrenees

I. Dorado Liñán et al.

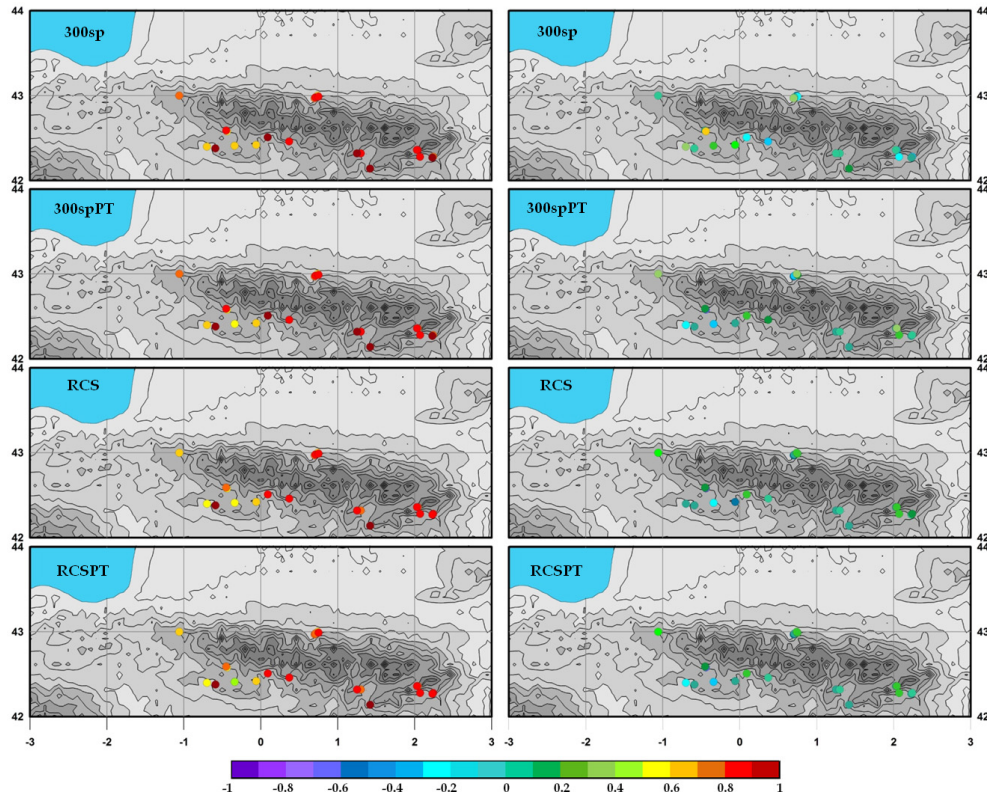


Fig. 4. EOF maps corresponding to the first and second principal component for each of the standardization methods used for building the site MXD chronologies: 300 sp, 300 spPT, RCS and RCSPT. The principal component analysis (PCA) was run for the common period 1928–1977.

[Title Page](#)[Abstract](#)[Introduction](#)[Conclusions](#)[References](#)[Tables](#)[Figures](#)[|◀](#)[▶|](#)[◀](#)[▶](#)[Back](#)[Close](#)[Full Screen / Esc](#)[Printer-friendly Version](#)[Interactive Discussion](#)

Cross-comparison at the Pyrenees

I. Dorado Liñán et al.

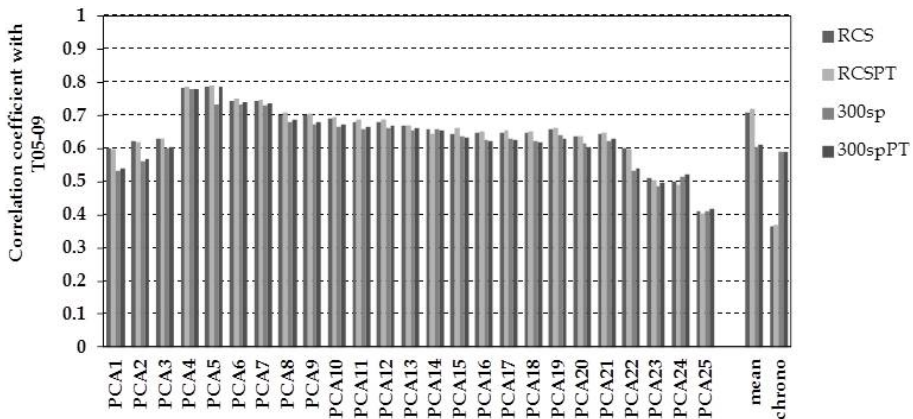


Fig. 5. Pearson's correlation coefficient of the PC1 of each PCA analysis (1 to 25), the regional chronologies *mean* and *chrono* and May to September mean temperature (T_{05-09}) for each standardization method (RCS, RCSPT, 300 sp, 300 spPT).

Title Page	Abstract	Introduction
Conclusions	References	
Tables	Figures	
◀	▶	
◀	▶	
Back	Close	
Full Screen / Esc		

Printer-friendly Version	
Interactive Discussion	



Cross-comparison at the Pyrenees

I. Dorado Liñán et al.

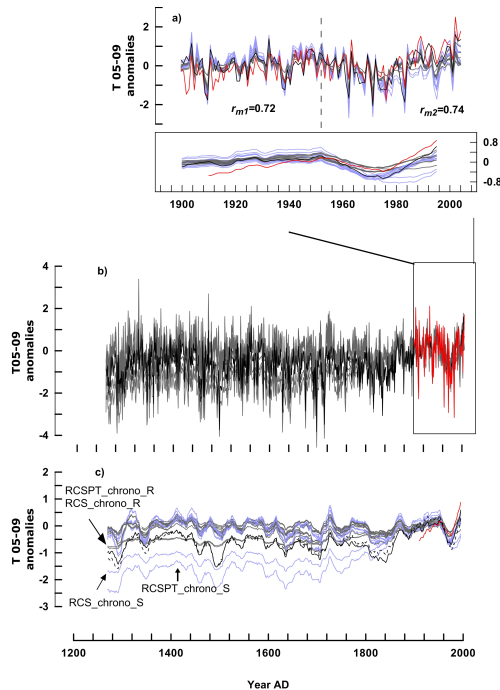


Fig. 6. May to September (T_{05-09}) mean temperature reconstructions. **(a)** Calibration-verification for the 24 different regional reconstructions performed by regression (grey lines) and scaling (blue lines), the mPYR (black line) and the instrumental May to September temperature record (red line). The bottom panel displays low-pass filtered series (20 yr moving average). Mean correlations (r_m) for the two split periods (1900–1952 and 1953–2005) are also shown. **(b)** Comparison between instrumental series, the 24 Pyrenees regional reconstructions and mPYR for the entire reliable period. **(c)** 20 yr low-pass filtered reconstructions and instrumental record. Dashed black line represents the original May to September maximum temperature reconstruction from Büntgen et al. (2008) (PYR).

Cross-comparison at the Pyrenees

I. Dorado Liñán et al.

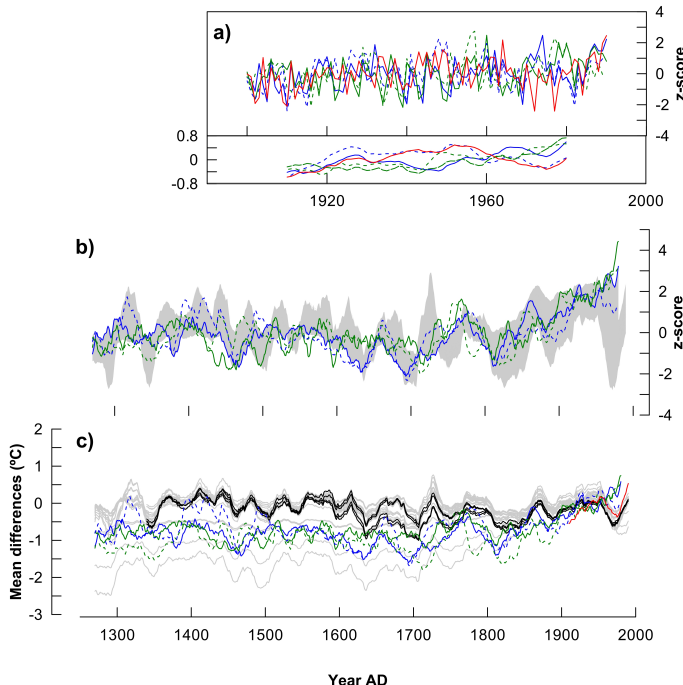


Fig. 7. Comparison of reconstructed and simulated May to September mean temperature for the last 750 yr. Grey lines/shade corresponds to the range of the 24 MXD based temperature reconstructions developed at the Pyrenees. Colored lines correspond to the different model outputs: Erik1 (blue), Erik2 (green), MM5-Erik1 (dashed blue) and MM5-Erik2 (dashed green). All series smoothed with a 20 yr centered moving average. **(a)** Comparison of the simulated May to September mean temperatures and the instrumental record (black line). **(b)** Series scaled to mean 0 and standard deviation 1. **(c)** Series in anomalies (differences from reference period 1900–2005). Black series correspond to the reconstructions PCs_RCS_S; PCs_RCSPT_S; PCs_300 sp_S and PCs_300 spPT_S.

[Title Page](#)

[Abstract](#)

[Introduction](#)

[Conclusions](#)

[References](#)

[Tables](#)

[Figures](#)

◀

▶

◀

▶

[Back](#)

[Close](#)

[Full Screen / Esc](#)

[Printer-friendly Version](#)

[Interactive Discussion](#)